Proceedings of Global Power and Propulsion Society
ISSN-Nr: 2504-4400
GPPS Xi'an21
18th – 20th October, 2021
www.gpps.global

GPPS-TC-2021-0131

THE INFLUENCE OF BACK PRESSURE CHANGE ON THE LEAKAGE FLOW CHARACTERISTICS OF THE LAST STAGE BLADE TIP CLEARANCE OF STEAM TURBINE

Yunyun Yuan
Department of Power Engineering,
North China Electric Power University
2932268218@qq.com
Baoding, People's Republic of China

Xu Han*
Hebei Key Laboratory of Low Carbon and High Efficiency Power Generation Technology,
North China Electric Power University
xuhan@ncepu.edu.cn
Baoding, People's Republic of China

Peng Li
Department of Power Engineering,
North China Electric Power University
pengli@ncepu.edu.cn
Baoding, People's Republic of China

Zhonghe Han
Department of Power Engineering,
North China Electric Power University
hanzhonghe@ncepu.edu.cn
Baoding, People's Republic of China

ABSTRACT

It is of great significance to fully understand the tip clearance leakage flow of rotor blades for improving the working efficiency of steam turbines. Taking the last stage of low pressure cylinder of a 600MW steam turbine as the research object, the tip clearance leakage flow of rotor blade under different outlet pressure was numerically simulated. The flow field characteristics and the influence of outlet pressure on the leakage flow were analyzed. The results show that there is obvious separation flow on the pressure surface and suction surface. On the pressure surface, with the increase of outlet pressure, the position of separation fluid gradually moves down. The positions of separation fluid in working conditions 1, 2 and 3 are 65%, 50% and 15%, respectively. In case 3, a small reflux vortex appears at the root of the pressure surface. On the suction side, there is an obvious separation vortex in case 1. In case 2 and 3, it can be clearly seen that the lower passage vortex is formed at the blade root. It is opposite to the separation fluid rotation direction, and the influence range increases with the increase of outlet pressure. At the same time, with the increase of outlet pressure, the pressure difference on both sides of the blade decreases, and the blocking effect of leakage flow on the main flow is weakened. When the outlet pressure is 15kPa, there is backflow at the top of rotor blade. It interacts with leakage flow and main flow to further increase the loss. The research has a certain reference value for the optimization of flow structure of steam turbine.

INTRODUCTION

When a steam turbine is designed and manufactured, there will be a gap between the top of the rotor blade and the cylinder wall. It is to prevent the damage of the components caused by the friction between the two during the operation of the steam turbine. However, there is a certain pressure difference between the pressure surface and the suction surface. Under the action of pressure difference, some fluid will flow from the high pressure side through the gap to the low pressure side, resulting in leakage loss. Moreover, the tip clearance leakage flow interferes with the main flow. It makes the downstream flow field unstable and increases the aerodynamic loss. In addition, tip clearance leakage will increase the complexity of blade heat transfer and shorten blade life. How to effectively reduce the leakage loss and improve the flow passage efficiency of steam turbine has always been a hot topic at home and abroad. Denton (1993) believed that the main cause of leakage loss was the interaction between leakage flow and main flow, and established the empirical formula and model of leakage loss based on experiments. Then, some scholars at home and abroad have carried out detailed research and analysis on the tip clearance leakage flow through numerical simulation method.

In recent years, Foreign scholar Tallman and Lakshminarayana (2000) considered the influence of tip clearance on leakage flow and vortex, and found that the decrease of tip clearance would lead to the decrease of mass flow through the clearance. Therefore, the strength of leakage vortex is reduced and the heat loss of gap and vortex is reduced. Palmer et al. (2016) based on the experimental study and numerical simulation of tip clearance leakage flow, the mechanism of leakage loss was quantitatively analyzed. On the basis of numerical study, Ong et al. (2012) analyzed the mixing process of leakage flow and mainstream flow, and considered that the fluid leakage can be reduced by increasing the swirl angle, so as to improve the efficiency. Domestic scholars Li et al. (2007) simulated the leakage flow under different tip clearance, analyzed the formation, development and loss of clearance flow and clearance vortex. The results show that with the increase of the gap, the location of leakage vortex is advanced, the leakage flow intensity is enhanced, and the flow loss is increased. Deng et al. (2007) used three-dimensional simulation method to study the tip clearance leakage flow into the turbine rotor blade. It is considered that the relative motion between the shroud and the rotor plays an important role in tip clearance leakage flow. In addition, (Deng et al., 2008)there is the influence of pressure difference between pressure surface and suction surface. In order to reduce the transverse flow effectively, the circumferential groove, axial groove or honeycomb are set on the surface of rotor exit shroud. Based on the idea of reducing tip clearance leakage of steam turbine, Li et al. (2009) simulated the influence of jet flow on tip clearance flow under two tip clearance heights. Analyzed the tip clearance flow structure, and calculated the efficiency of steam turbine considering the influence of jet flow. Yang et al. (2010) numerically studied the effect of rotation on tip leakage flow and heat transfer, and considered that the relative motion of the shroud was the main factor. In addition, Li et al. (2011) also conducted steady and unsteady numerical analysis on the leakage flow and heat transfer characteristics at the tip of the rotor blade. It is considered that there are two vortices in the tip clearance, and these two vortices have a certain influence on the local heat transfer characteristics of tip clearance. Gao et al. (2017) conducted a numerical study on the development pattern of leakage vortex, and analyzed the interaction between leakage vortex and mainstream passage vortex in detail. Cao et al. (2014) analyzed the influence of clearance size on the turbine tip clearance leakage vortex through numerical simulation, studied the influence of clearance leakage on the relative internal efficiency and power of the turbine, and calculated the related leakage loss (2019). It is considered that the leakage loss is mainly related to the radial clearance, and all the loss coefficients will increase with the increase of tip clearance. In addition, with the increase of clearance, the output loss increases and the relative internal efficiency of stage decreases linearly. The research object of the existing literature is mostly the high-pressure cylinder of steam turbine. Its blade passage working fluid is superheated steam. At present, there is little literature on tip clearance leakage flow in wet steam stage of steam turbine. There is condensation in the wet steam stage, which will also affect the performance of the steam turbine. In this paper, the last stage of the low pressure cylinder of a 600MW turbine is selected as the research object. The flow field characteristics of tip clearance leakage flow of rotor blades under different outlet pressures were studied by numerical calculation method. And the influence of outlet pressure on leakage flow was analyzed.

METHODOLOGY

Numerical Methods

In this paper, a homogeneous media multiphase model is used to solve tip clearance leakage flows. The model considers that in a given transport process, all transport quantities except volume fraction are the same for all phases. And the model assumes that there is no slip between each phase. Therefore, its continuity equation can be expressed as:

$$\frac{\partial}{\partial t}\left(r_\alpha \rho_\alpha\right)+\nabla\cdot\left(r_\alpha \rho_\alpha U\right)=S_{MS\alpha}+\sum_{\beta=1}^{N_P} M_{\alpha\beta} \quad . \quad (1)$$

Where α and β represent phases in the fluid working medium. r_α represents the volume fraction of phase α. ρ_α denotes the density of phase α, kg/m^3. U stands for speed, m/s. $S_{MS\alpha}$ represents a customizable quality source item. $M_{\alpha\beta}$ represents the mass flow rate per unit volume of phase β to phase α. N_p is the total number of phases.

The momentum equation is as follows:

$$\frac{\partial}{\partial t}(\rho U)+\nabla\cdot\left\{\rho UU-\mu\left[\nabla U+(\nabla U)^T\right]\right\}=S_M-\nabla p \quad . \quad (2)$$

In the formula, S_M represents the momentum source term that can be customized.

The energy equation is as follows:

$$\frac{\partial}{\partial t}(\rho H)-\frac{\partial P}{\partial t}+\nabla\cdot(\rho UH)=\nabla\cdot(\lambda\Delta T)+S_E \quad . \quad (3)$$

In the formula, S_E represents the energy source term that can be customized.

In the last stage channel of a steam turbine, the flow state of its working fluids is mainly turbulent flow. Turbulence is a kind of disordered flow, showing the characteristics of three-dimensional unsteady and rotating distribution. The standard model k-ε can simulate the turbulent flow far away from the wall, and it can meet the requirements of complex flow research in the channel. Therefore, k-ε equation is selected as the turbulence model in this paper. The equation is expressed as follows:

$$\frac{\partial(\rho k)}{\partial t}+\frac{\partial(\rho k u_i)}{\partial x_i}$$
$$=\frac{\partial}{\partial x_j}\left[\left(\mu+\frac{\mu_t}{\sigma_k}\right)\frac{\partial k}{\partial x_j}\right]+G_k+G_b-\rho\varepsilon-Y_M+S_k \quad . \quad (4)$$

$$\frac{\partial(\rho k)}{\partial t}+\frac{\partial(\rho\varepsilon u_i)}{\partial x_i}$$
$$=\frac{\partial}{\partial x_j}\left[\left(\mu+\frac{\mu_t}{\sigma_\varepsilon}\right)\frac{\partial \varepsilon}{\partial x_j}\right]+C_{1\varepsilon}\frac{\varepsilon}{k}\left(G_k+C_{3\varepsilon}G_b\right)$$
$$-C_{2\varepsilon}\rho\frac{\varepsilon^2}{k}+S_\varepsilon \quad . \quad (5)$$

Where G_k and G_b are the generation terms of turbulent kinetic energy k caused by average velocity gradient and buoyancy respectively. $C_{1\varepsilon}$、$C_{2\varepsilon}$ and $C_{3\varepsilon}$ are the empirical constant. Y_M is the expansion of pulsation in compressible turbulence. σ_k is the Prandtl number corresponding to the turbulent kinetic energy k. σ_ε is the dissipation rate ε Corresponding Prandtl number. S_k and S_ε are the source item. u_i represents time average speed. μ_t is turbulent viscosity.

Based on the above model, the finite volume method is used to solve the three-dimensional compressible steady-state Reynolds averaged Navier Stokes equations. Turbulence model selection k-ε in the equation, scalable wall function is selected for the basin near the wall of rotor and rotor blades, and high-order upwind scheme is selected for convection term. The steam3vl model in IAPWS-IF97 is used as the mobile working fluid. The runner is set to periodic boundary conditions. In actual operation, the rotating speed of the rotor cascade is stable, and the loss caused by the relative change of the position between the stator-rotor interface is small. It is considered that the flow process belongs to the category of quasi steady state flow. Therefore, the Frozen Rotor model is used to realize the numerical transfer of the stator-rotor interface. The boundary conditions are set as mass inlet and average static pressure outlet. The calculated boundary conditions are shown in Table1.

In addition, in order to verify the accuracy of the numerical model in this paper, the numerical simulation results of inlet mass flow of 67.783kg/s, temperature of 335.05K, humidity of 0.0549 and outlet average static pressure of 4.9kPa are compared with the measured results of steam turbine performance test. As shown in Table 2. The absolute value of the relative error between the numerical results and the test results is less than 5%. The reliability of the numerical model, calculation model and calculation results are verified.

Table 1 Boundary Conditions of Various Working Conditions

Parameter / Case	Inlet conditions			Oulet conditions
	Total temperature/(K)	Mass flow rate /(kg/s^{-1})	Pressure /(kPa)	Pressure /(kPa)
1	335.05	67.783	19.353	5
2			20.038	10
3			21.357	15

Table 2 Comparison Between Test Results and Numerical Calculation Results

Parameter	Test results	Numerical results	Relative error/%
Inlet pressure/kPa	21.8	21.18	2.84
Inlet temperature/℃	61.9	60.06	2.97
Static pressure difference/kPa	10.1	10.38	-2.77
Whole stage differential pressure/kPa	16.9	16.38	3.08
Outlet temperature/℃	36.2	35.70	1.38

Physical Model

Taking the last stage of low pressure cylinder of 600MW supercritical steam turbine unit as the research object, the three-dimensional numerical calculation of blade flow field is carried out by using commercial software ANSYS CFX 17.0. Figure 1 shows the simplified last stage blade. The last stage has 52 stator blades and 80 rotor blades. The height of the rotor blade is 1029mm, the height of the stator blade is 953mm. The top of the stator blade is inclined at 45 degrees, the clearance between the rotor and stator blade is 115.2mm. The clearance between the top of the rotor blade is 11.2mm, and the rotating speed is 3000r/min. TurboGrid 17.0 is used to divide the final level area into structured grid, and its topology is "HOH". The "H" type orthogonal grid is used at the inlet and outlet of the cascade and the tip clearance. Considering the influence of boundary layer flow on the whole flow field, the grid near the wall of the last stage watershed is densified. In order to prevent the deterioration of the calculation results, the value of Y+ near the wall of the rotor and stator blade is limited within the range of 30-300. The grid diagram at the top of the cascade is shown in Figure 2.

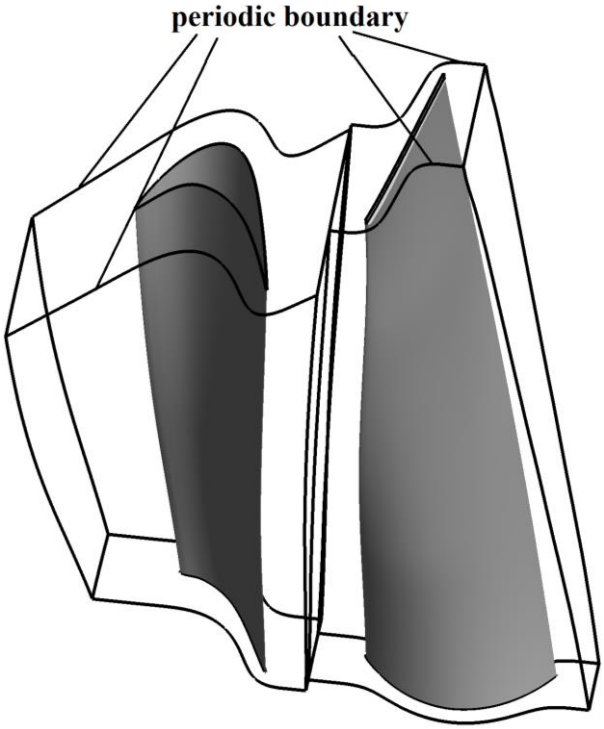

Figure 1 Final Stage Model of Steam Turbine

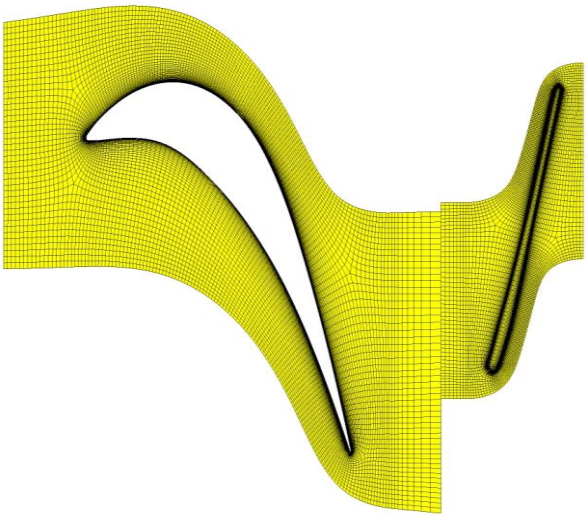

Figure 2 Grid Diagram of Last Stage Blade

Verification of Grid Independence

In order to eliminate the influence of the number of grids on the calculation results, the grid independence is verified in this paper. Four sets of grids with the same topology of 0.8 million, 1.6 million, 2.1 million and 2.8 million are used for numerical calculation, as shown in Figure 3. It is found that with the increase of the number of grids, the relative deviation of blade surface pressure decreases gradually. When the number of grids is more than 2.1 million, the calculation results will not change. Therefore, it is considered that the number of 2.1 million grids meets the requirement of independence, and this number is used in this paper.

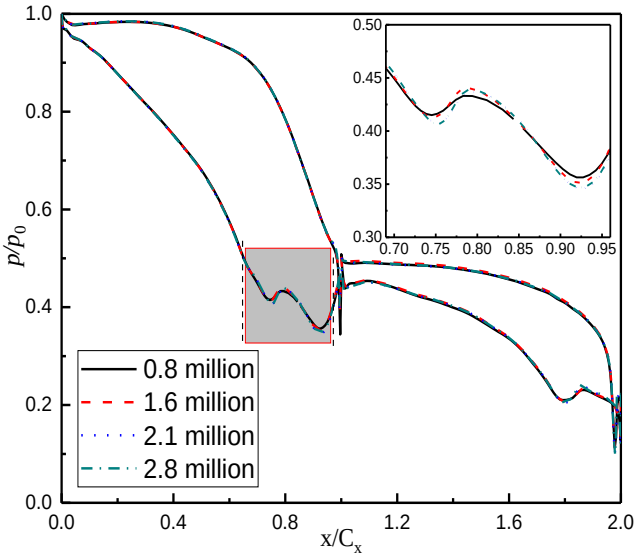

Figure 3 Grid Independence Verification

RESULTS AND DISCUSSION

Limiting Streamline Distribution under Different Working Conditions

The material surface is a zero flow surface, when the velocity on the viscous material surface is zero, there is no streamline on it. The streamline close to the material surface is defined as the limiting streamline (Tong et al., 1993). Figure 4 is the limit flow diagram of the final rotor blade surface under different working conditions.

As shown in Figure 4, in all working conditions, there are obvious separated flows on both sides of the pressure surface and suction surface of the rotor blade. The position of the separation flow on the pressure surface is gradually moved downward due to the increase of the outlet pressure. In case 1, the separation flow occurs near 65% of the blade height. In case 2, the separation flow occurs at 50% of the blade height. And in case 3, the separation flow occurs at 15% of the blade height. While the separating fluid obstructs the mainstream flow, its own flow will also be crowded out by the mainstream. Under this interaction, the separation fluid develops gradually towards the tip of the blade. And with the increase of outlet pressure, more separation fluid flows to the tip direction. In addition, a small reflux vortex appears at the root of the pressure surface in case 3. The phenomenon of flow separation also appears at the root of the suction surface, and there is an obvious separation vortex in case 1. In case 2 and case 3, it is obvious that there is a lower passage vortex opposite to the separation vortex near the blade root, which develops along the axial direction and gradually expands. In case 2, the vortex in the lower passage develops upward along the suction direction, and finally flows out of the passage at 20% of the blade height. In case 3, the vortex in the lower passage flows out from 50% of the blade height. The existence of the vortex in the lower passage will reduce the rotor load and affect the flow efficiency of the last stage of the steam turbine. And the influence range

of the vortex in the lower passage will increase with the increase of the outlet pressure.

(a) case 1 (b) case 2 (c) case 3

Pressure surface

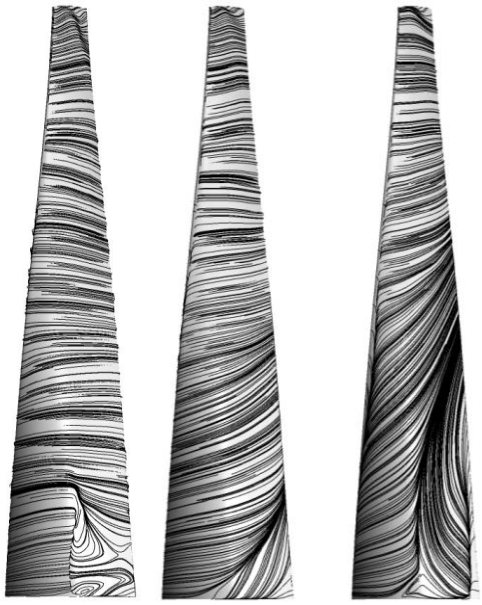

(a) case 1 (b) case 2 (c) case 3

Suction surface

Figure 4 Limit Flow Diagram of Rotor Blade Surface

Tip Pressure Distribution

Figure 5 shows the influence of rotor blade outlet pressure on blade tip pressure. In all cases, the pressure on the pressure surface at the blade tip inlet is less than that on the suction surface. This is due to the inlet steam flow at the top of the blade flowing into the cascade at a negative angle of attack. After 10% axial position, the pressure on the pressure surface is higher than that on the suction surface. And the pressure difference between them makes the fluid flow from the high pressure side to the low pressure side through the tip clearance, resulting in leakage loss. In addition, the pressure difference on both sides of the blade between 20% axial position and 90% axial position presents an upward-gentle-downward trend. When the outlet pressure is 5kPa, the pressure difference between the two sides of the blade reaches to about 9000 Pa. When the outlet pressure is 10kPa, the pressure difference is the highest of 6000Pa. When the outlet pressure is 15kPa, the pressure difference between the two sides of the blade changes gently, and the maximum difference is 3000Pa. In general, with the increase of outlet pressure, the pressure difference between the two sides of the blade tip gradually decreases. Thus weakening the strength of the leakage flow and reducing the leakage loss.

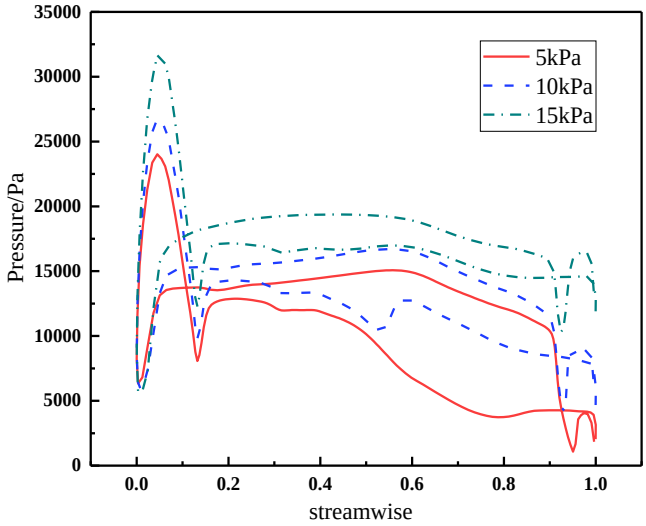

Figure 5 Influence of Outlet Pressure on Tip Pressure

Velocity Distribution of 50% Axial Section and Outlet Section of Rotor Blade

Figure 6 shows the distribution of 50% axial section velocity along blade height under different outlet pressures. It can be seen from Figure 6 that when the outlet pressure is 5kPa, the main flow velocity from the blade root to 40% of the blade height decreases greatly. Combined with Figure 4, it can be found that this is caused by the separation fluid near the blade root hindering the mainstream flow. From 40% of the height to the top of the blade, the mainstream velocity no longer decreases, but increases slowly. When the outlet pressure is 10kPa, the main flow velocity decreases gradually from the blade root to about 30% of the blade height, and then increases slowly. When the outlet pressure is 15kPa, the main flow velocity increases all the time from the blade root to the blade tip, but the increasing range of velocity is different. Under the three conditions, the growth rate of mainstream velocity from 90% blade height to blade top is lower than that in the previous stage. This shows that the leakage flow hinders the main

flow, which reduces the flow capacity of the main flow. In addition, with the increase of the outlet pressure, the growth rate of the main flow velocity near the blade tip decreases. It shows that the change of working condition makes the intensity of leakage flow weaken and the loss decrease. Figure 7 shows the velocity distribution of the rotor blade exit section. Similarly, at about 90% of the blade height to the tip, the increase of fluid velocity has a similar change as that in Figure 6. Especially, when the outlet pressure is 15kPa, the main flow velocity at the blade tip decreases slightly, and it is possible that there is backflow at the blade tip.

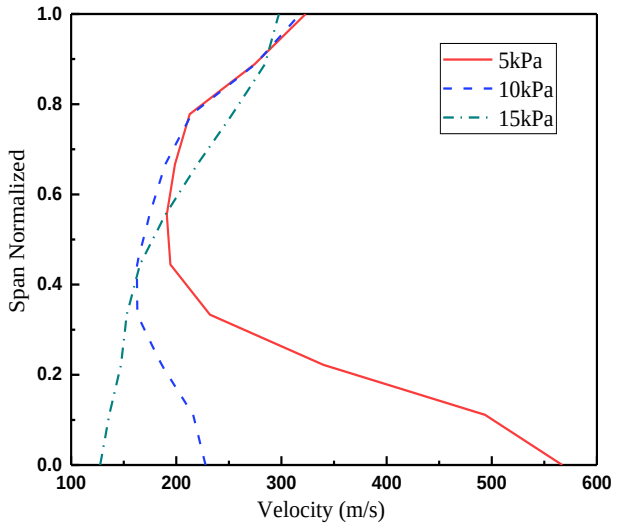

Figure 6 Velocity Distribution at 50% Axial Section

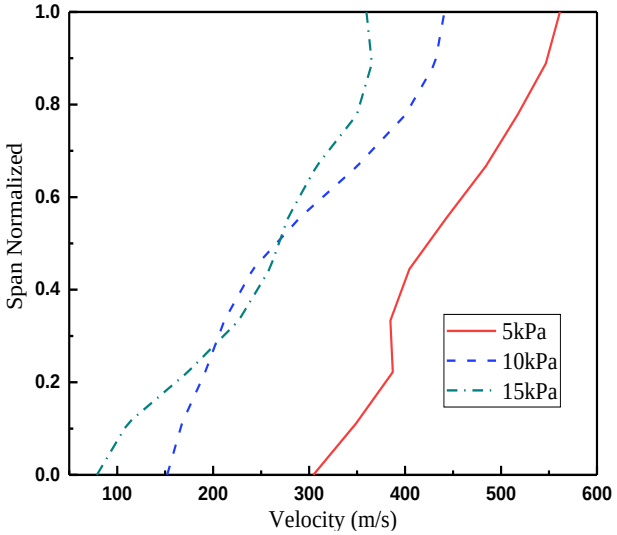

Figure 7 Velocity Distribution at The Exit Section

Outlet Steam Flow Angle Distribution under Different Working Conditions

Figure 8 shows the distribution of steam flow angle at rotor blade outlet. Its definition is as follows:

$$\beta = \arctan\left(V_y / V_x\right). \quad (6)$$

Where β represents the outlet steam flow Angle, °. V_y represents the axial velocity component at the rotor blade outlet, m/s. V_x represents the velocity component of the rotor blade outlet along the pitch direction, m/s.

The steam flow in the cascade passage has been fully developed when it reaches the outlet section of the rotor blade. It can be seen from Figure 8 that there is a small vortex near the tip of the blade under all working conditions. This is caused by the interaction between the leakage flow and the main flow. And its blocking effect on the main flow will increase the flow loss of the rotor blade to a certain extent. In addition, it can be observed that the outlet steam flow angle of tip leakage vortex region is larger in all conditions. In case 1, the maximum outlet steam flow angle can reach 70 °, the steam flow angle at the leakage vortex reaches 60 °in case 2, condition 3 reaches 55 °. However, the outlet steam flow angle decreases significantly from the blade height down to the middle of the blade. At this time, the outlet steam flow angle of all working conditions basically plummets to about 20°, and the lowest reaches 5°. This is caused by the interference of the upper passage vortex. The outlet steam flow angle of the blade root changes in different degrees under the action of the separated fluid. By comparing the three working conditions, it can be concluded that: the outlet steam flow angle decreases with the increase of outlet pressure, and changes obviously in the tip region. This is due to the increase of outlet pressure and the decrease of tip pressure difference. Therefore, the intensity of leakage flow is weakened and the steam flow angle at the top of blade is affected.

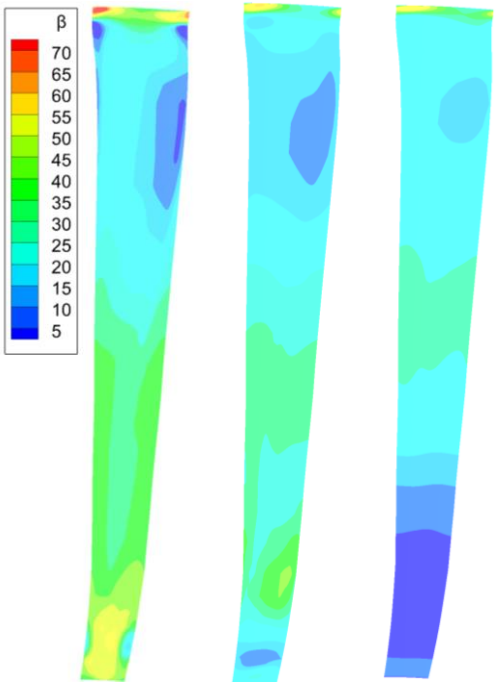

(a) case 1 (b) case 2 (c) case 3

Figure 8 Outlet Steam Flow Angle

Distribution of Pressure Loss Coefficient of Rotor Blade Outlet Section

The total pressure loss coefficient can be used to characterize the energy loss of fluid in the process of flow (Cao et al., 2013). Its definition is as follows:

$$C_{pt} = \frac{P_0 - P_1}{\frac{1}{2}\rho\overline{U}^2} \quad . \quad (7)$$

Where, P_0 represents the total pressure at the rotor blade inlet, Pa. P_1 represents the total pressure at the outlet section of the rotor blade, Pa. ρ represents the density of steam at the inlet of the rotor blade, kg/m^3. U represents the average velocity at the inlet of the rotor blade, m/s.

The loss of the upper half of the rotor blade is mainly caused by the mixing of the upper passage vortex and the leakage vortex and the entrainment of low energy fluid. In Figure 9, the upper part of the outlet section is selected for the total pressure loss analysis, and the existence of tip leakage vortex can also be seen from the figure. With the increase of outlet pressure, the loss caused by the interaction between leakage vortex and upper passage vortex changes. Compared with condition 2 and 3, the total pressure loss coefficient of condition 1 decreases with the change of condition, the interference effect of leakage flow on the main flow weakens, and the loss decreases accordingly. However, the total pressure loss coefficient at the top of blade in condition 3 is slightly larger than that in condition 2. This may be due to the backflow at the outlet of condition 3. The backflow interacts with the leakage flow and the main flow to increase the loss.

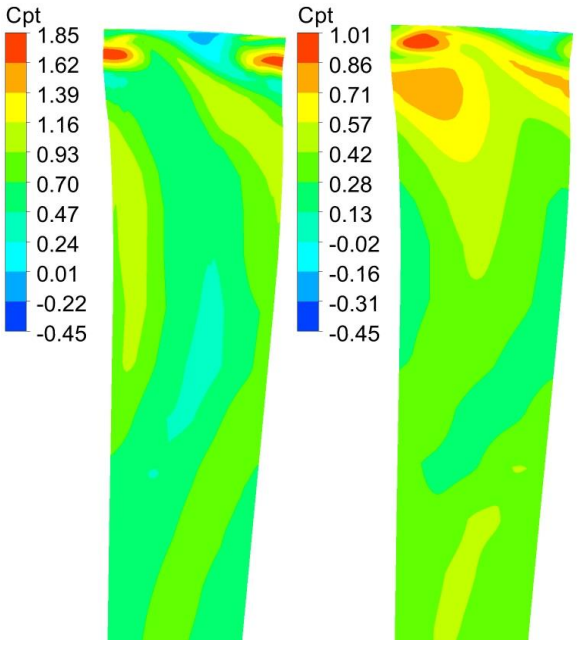

(a) case 1 **(b) case 2**

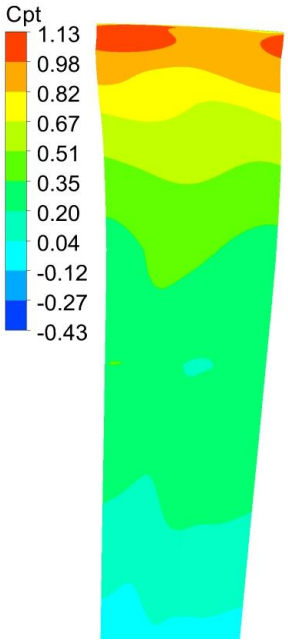

(c) case 3

Figure 9 Pressure Loss Distribution of Rotor Blade Outlet Section

CONCLUSIONS

The pressure difference between the suction surface and the pressure surface of the rotor blade causes part of the fluid to deviate from the main flow direction. It flows from the high pressure side to the low pressure side through the tip clearance, causing leakage loss and reducing the flow efficiency. In this paper, the leakage flow in the tip clearance of wet steam stage of steam turbine is numerically simulated. The flow field characteristics and the influence of outlet pressure on the leakage flow were analyzed. The results show that there is an obvious separation flow between the pressure surface and the suction surface. On the side of pressure surface, the position of separated fluid changes with the change of outlet pressure. The positions of separation fluid in working conditions 1, 2 and 3 are 65%, 50% and 15%, respectively. The position of the separated fluid is developing towards the tip of the blade. In case 3, a small reflux vortex appears at the root of the pressure surface. On the side of suction surface, there is an obvious separation vortex in case 1. In case 2 and 3, it can be clearly seen that the lower passage vortex is formed at the blade root. It is opposite to the rotation direction of the separation fluid, and the influence range increases with the increase of outlet pressure. At the same time, increasing the outlet pressure will reduce the pressure difference on both sides of the blade. This weakens the interference of leakage flow to the main stream to a certain extent. In addition, when the outlet pressure is 15kPa, there is backflow at the top of the rotor blade. It interacts with leakage flow and main flow to increase the loss.

ACKNOWLEDGEMENTS

The authors are thankful for the support provided by the National Natural Science Foundation of China (52106042), Natural Science Foundation of Hebei Province, China (grant number E2020502001), and the Fundamental Research Funds for the Central Universities of China (grant number 2019MS092).

DISCLOSURE STATEMENT

No potential conflict of interest was reported by the author(s).

REFERENCES

Denton, J. (1993). The 1993 IGTI Scholar Lecture: Loss Mechanisms in Turbomachines. *Journal of Turbomachinery*, 115(4), pp.621-656. Doi: 10.1115/1.2929299.

Tallman, J. and Lakshminarayana, B. (2000). Numerical Simulation of Tip Leakage Flows in Axial Flow Turbines, With Emphasis on Flow Physics: Part I —Effect of Tip Clearance Height. *Journal of Turbomachinery*, 123(2), pp.314-323. Doi:10.1115/1.1368881.

Palmer, T., Tan, C., Zuniga, H., Little, D., Montgomery, M. and Malandra, A. (2016). Quantifying Loss Mechanisms in Turbine Tip Shroud Cavity Flows. *Journal of Turbomachinery*, 138(9). Doi:10.1115/1.40329 22.

Ong, J., Miller, R. and Uchida, S. (2012). The Effect of Coolant Injection on the Endwall Flow of a High Pressure Turbine. *Journal of Turbomachinery*, 134(5),pp.915-924. Doi:10.1115/1.4003838.

Li, J., Lu, Q. and Feng, Z. (2007). Numerical Simulation of the Aerodynamic Characteristics of Blade Tip Leakage Flow in Steam Turbines. *Journal of Power Engineering*,(3),pp.314-317. Doi:10.1016/S1001-8042(07)60056-6.

Deng, Q., Niu, J. and Feng, Z. (2007). Tip Leakage Flow in Radial Inflow Rotor of a Microturbine With Varying Blade-Shroud Clearance. *Proceedings of the Asme Turbo Expo*,pp.1081-1088. Doi: 10.1115/GT2007-27722.

Deng, Q., Niu, J. and Feng, Z. (2008). Study on leakage flow characteristics of radial inflow turbines at rotor tip clearance. Science in China Series E: *Technological Sciences*, 51(8), pp.1125-1136. Doi:10.1007/s114 31-008-0164-z.

Li, W., Qiao, W., Xu, K. and Luo, H. (2009). Numerical Simulation of Active Control on Tip Leakage Flow in Axial Turbine. *Chinese Journal of Aeronautics*, 22(2), pp.129-137. Doi:10.1016/s1000-9361(08)60078-3.

Yang, D., Yu, X. and Feng, Z. (2010). Investigation of Leakage Flow and Heat Transfer in a Gas Turbine Blade Tip With Emphasis on the Effect of Rotation. *Journal of Turbomachinery*, 132(4). Doi: 10.1115/1.3213560.

Li, J., Sun, H., Wang, J. and Feng, Z. (2011). Numerical investigations on the steady and unsteady leakage flow and heat transfer characteristics of rotor blade squealer tip. *Journal of Thermal Science*, 20(4), pp.304-311. Doi:10.1007/s11630-011-0474-5.

Gao, J., Wang, F., Fu, W., Yue, G., Zheng, Q. and Dong, P. (2017). Experimental Investigation of Effects of Tip Cavity on Tip Clearance Flow in a Variable Geometry Turbine Cascade. *Journal of Aerospace Engineering*, 30(1), p.04016069. Doi:10.1061/(asce)as. 1943-5525.0000656.

Cao, L. (2014). Numerical Analysis of Tip Leakage Flow in Steam Turbine Rotor Cascades. *Journal of Mechanical Engineering*, 50(4), p.172. Doi:10.3901/jme.2014.04.172.

Cao, L., Si, H., Wang, J. and Li, P. (2019). Effects of leakage vortex on aerodynamic performance and loss mechanism of steam turbine. Proceedings of the Institution of Mechanical Engineers, Part A: *Journal of Power and Energy*, 233(7), pp.866-876. Doi:10.1177/0957650919831916.

Tong, B., Zhang, B. and Cui, E. (1993). *Unsteady flow and vortex motion*. Beijing: National Defense Industry Press.

Hu, P., Cao, L., Li, Y. (2013). Tip Clearance Impact on Tip Leakage Flow in Steam Turbine. *Chemical Engineering & Machinery*,40(5),pp.628-633. Doi:10.3969/j.issn.0254-6094.2013.05.020.